*Egypt. J. Chem.* **Vol. 66,** No. 3 pp. 259 – 263 (2023)

**Egyptian Journal of Chemistry**

**http://ejchem.journals.ekb.eg/**

# Uv-Irradiation Synthesized $Co_3ZnFe_2O_8$ Nanoparticles For Corrosion Protection Of Carbon Steel In Seawater

**Riyam L.Khalaf[1], Israa M. H. Almousawi[1], Ahmed Mahdi Rheima[*2]***

[1]*Department of Chemistry, College of Science, University of Baghdad, Iraq*
[2] *Department of Chemistry, College of Science, Mustansiriyah University, Baghdad, Iraq*

**Abstract**

A novel trinary $Co_3ZnFe_2O_8$ nanoparticle was synthesized using a photo-irradiation method with different solvents (water, chloroform, methanol, and ethanol). The $Co_3ZnFe_2O_8$ nanoparticles were investigated by scanning and transmission electron microscopy measurements (SEM), Atomic force microscopy (AFM), and their crystal structure was obtained by the X-ray diffraction technique (XRD). The investigated results show that the Average size of $Co_3ZnFe_2O_8$ nanoparticles ranges from 35 to 103 nm by different solvents. The X-ray diffraction proved the cubic shape of the prepared nano-samples with an average crystal size ranging from 8 to 22 nm. The $Co_3ZnFe_2O_8$ nanoparticles were applied as a coating for corrosion protection of carbon steel in seawater. Finally, The corrosion production was equal to 74% at 298 K. It can be concluded that the prepared nanoparticles are highly effective in the protection

***Keywords*:** $Co_3ZnFe_2O_8$ nanoparticles, photo-irradiation method, carbon steel, seawater;

## 1. Introduction

In various technical applications, particulates are utilized to make biosensors, antiviral, microelectronic circuits, antibacterial, anticancer, fuel cells, piezoelectric devices, and catalysts and corrosion inhibitors. One of the goals of the growing science of nanotechnology is to create nanostructures and nanoscales with unique properties in terms of bulk or specific particles [1, 2]. Because of the small size and high surface area, nanocomposites have individual chemicals and physical properties. The oxide nanocomposite properties arise due to the structural peculiarities of these compounds, precisely the point defects that give rise to semiconducting nature[3, 4]. The concept behind nanocomposite is to produce and design a new material with unprecedented flexibility and devolvement in physical and chemical properties using building blocks with diameters in the nanometer (less than 100 nm) range. A nanocomposite is a solid material with more than one phase. Each has one, two, or three dimensions of less than 100 nanometers (nm) or structures with nanoscale repetitive intervals between the components that make up the produc[5]. Cobalt oxide and zinc oxide iron oxides are well-known magnetic materials used in electrical equipment and microwave devices[6, 7]. Because of the high electrical resistivity and magnetic softness, nanocomposites' core loss is minimal when used with high-frequency inductors or transformers [8]. Cobalt oxide is electromagnetic. With a large saturation magnetization and a high Snoek's limit, zinc oxide iron oxides with good mechanical hardness and chemical stability have highly complicated permeability values over a wide frequency range. Because of the preceding, cobalt-zinc iron is an excellent thin absorber for high-frequency applications[9]. Electrophoretic depositions (EPD) are a quick technique for depositing nanocomposite on an electrode utilizing a stable solution in a DC field. Electrophoretic deposition (EPD) is coating nanocomposite on carbon steel surfaces. EPD is a straightforward method for forming a coating nanocomposite on an electrode using a stable solution in a direct current (DC) field[10, 11]. This study aims to examine the efficiency of nanocomposite to protect Carbon steel (C.S) from corrosion using absolute ethanol as a suspension medium[12- 14]. In this project, photolysis presses were adopted to synthesize novel trinary $Co_3ZnFe_2O_8$ nanocomposite for corrosion protection of carbon steel in seawater.

### Experimental

All of the chemicals were bought from the same place (BDH, Merck, and Sigma-Aldrich); figure 1 shows the irradiation cell utilized to irradiate cobalt, zinc, and iron salt as nanoparticles sources. 125-watt

*Corresponding Author: arahema@uowasit.edu.iq.; (Riyam L. Khalaf).
Receive Date: 04 March 2022, Revise Date: 21 April 2022, Accept Date: 18 July 2022
DOI: 10.21608/EJCHEM.2022.125402.5577

mercury medium pressure lamps with high maximum light intensity at 365 nm are employed in the submerged UV source. In the complicated solution of nanoparticles, the cell has a quartz tube like a jacket for an immersion UV source. As the reactor, a Pyrex tube was employed. The reactor was cooled using an ice bath to avoid the temperature rise due to the UV irradiation.

Synthesis of trinary $Co_3ZnFe_2O_8$ nanoparticles by different solvents 150 ml, 0.01 mole $Na_3Co\ (NO_2)_6$ was mixed with 150 ml, 0.01 mole Zn $(CH_3COO)_2$ and with 150 ml, 0.01 mole FeC2O4.H2O as a mole ratio (1:1:1). Then, 150 ml, 0.03 mole of urea was slowly added (drop by the second) to the mixture and stirred for 10 min. After that, a photocell is used to irradiate the solution for 30 minutes while freezing it to 5 degrees Celsius. The trinary superposition is precipitated as a brown powder, separated, and washed multiple times (all steps done with centrifuge then decantation)[9]. The residue was dried for one hour at 100°C before calcining for three hours at 300°C. $Co_3ZnFe_2O_8$ nanoparticles with a black-brown powder have been produced. The same procedure steps were performed in different solvents (water, chloroform, methanol, and ethanol) to dissolve and wash[15].

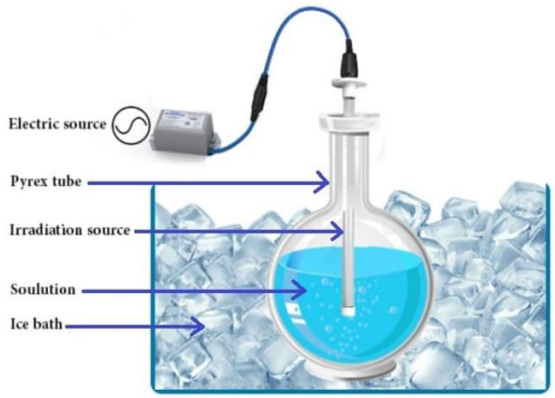


**Fig. 1. shows photo-irradiation cell**

**Corrosion protection study:** Emulsion solution was prepared by adding 1% $Co_3ZnFe_2O_8$ nanoparticles powder (prepared as a water solvent ) to ethanol as solvent (adding 1.5 g nanoparticles to 150 ml ethanol). The emulsion solutions were applied to study the protection of carbon steel (C45) pieces by coating them with nanoparticles using the EPD technique method. [16]. Electrophoresis Deposition of $Co_3ZnFe_2O_8$ nanoparticles as Emulsion Solution (Coating Samples).

A deposition cell device was utilized to cover $Co_3ZnFe_2O_8$ nanoparticles on stainless steel surfaces. The working electrode (Stainless steel) and a flat titanium sheet as a counter electrode were immersed in an electrolyte. Electrophoretic deposition of nanoparticles on the stainless steel was carried out at room temperature using a stirrer powered by a direct current (15 V). After deposition, the samples were washed in distilled water with a blow dryer[17].

**Result:**

**x- ray diffraction:**

XRD was used to study the crystal structure of prepared $Co_3ZnFe_2O_8$ Nanoparticles as calcination at 300 C˚ with different solvents ( **A.** water, **B.** chloroform, **C**. methanol, and **D**. ethanol ). Figure 2 shows the XRD pattern of the samples has a substantial number of broadening lines. The Debye-Scherrer formula was used to calculate the crystalline size [8]. The mean crystal sizes of nanoparticles are presented in table (1) [18]. When used a different solvent with a decrease in polarity; water(1), methanol(0.76), ethanol (0.65), and chloroform (0.23),

due to the increase in polarity cause a decrease in surface tension; the crystalline size of nanoparticle preparation increased with decrease with a polarity which prepares nanocomposite with large size. So the favorite solvent is water. The crystallite size of $ZnCo_3Fe_2O_8$ nanocomposite was 8.6 nm using water as solvent,12.2 as methanol solvent ,9.5 as ethanol solvent and 14.2 using choloroform as solvent.

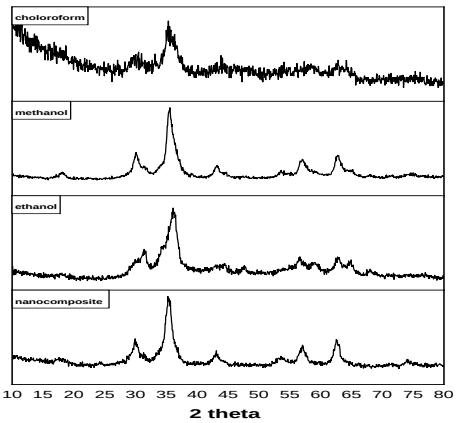


**Figure (2): XRD patterns of $Co_3ZnFe_2O_8$ Nanoparticles as solvents A. water, B. chloroform, C. methanol, and D. Ethanol.**

The prominent peaks were observed at 2θ values of 30°, 35.5°, 37°, 44°, 54°, 56°, 64°,72°,74°,75°,79°, and 82° were assigned (220), (311), (222), (400), (422), (511), (440), (620), (533), (622), (444) and (551) planes.

**Atomic force microscope (AFM):**

The particles size of nanocomposite and morphology were determined by an atomic force microscope (AFM). AFM images of the samples with different solvents were used to determine the particles' mean particle size and distribution. Figure 3 displays AFM images of the samples[19]. The average particle sizes were calculated using the AFM images presented in Table 1. (2).

**Table (1) the crystal size and crystal system of $Co_3ZnFe_2O_8$ Nanoparticles.**

| sample | phase | Crystal system | 2θ (deg) | crystal size (nm) |
|---|---|---|---|---|
| A | $Co_3ZnFe_2O_8$ | cubic | 35.4 | 8.6 |
| B | $Co_3ZnFe_2O_8$ | cubic | 35.3 | 14.2 |
| C | $Co_3ZnFe_2O_8$ | cubic | 36.3 | 9.5 |
| D | $Co_3ZnFe_2O_8$ | cubic | 35.4 | 12.2 |

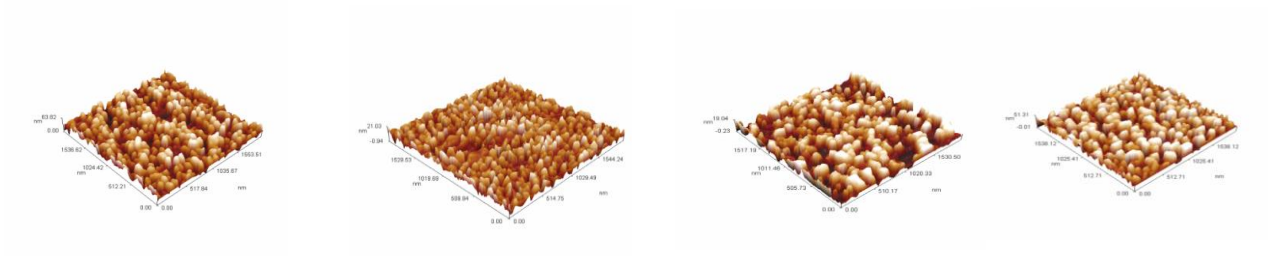

**Figure (3) AFM images of $Co_3ZnFe_2O_8$ Nanoparticles as solvents A. water, B. chloroform, C. methanol, and D. Ethanol.**

**Table (2) average particle size from AFM images**

| sample | phase | Average particles size (nm) |
|---|---|---|
| A | particle | 79 |
| B | Particle | 103 |
| C | Particle | 96.4 |
| D | Particle | 77.3 |

**Table (3) Average particle size from SEM**

| sample | phase | Average particles size (nm) |
|---|---|---|
| A | Nanocomposite | 69.5 |
| B | Nanocomposite | 54.5 |
| C | Nanocomposite | 54 |
| D | Nanocomposite | 54.9 |

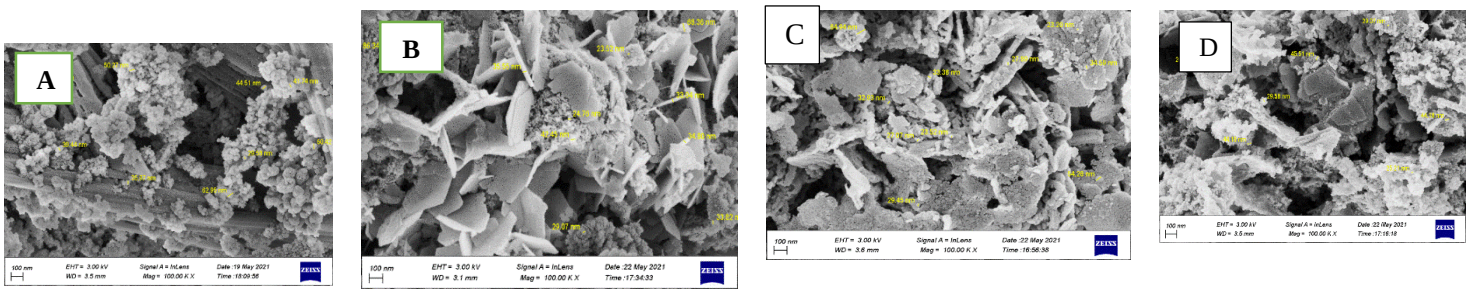


**Figure (4) SEM images of $Co_3ZnFe_2O_8$ Nanoparticles as solvents A. water, B. chloroform, C. methanol, and D. Ethanol.**

**Scanning electron microscope (SEM):**

The form and size distribution of nanocomposite is depicted in SEM images in figure (4). Nanocomposite surfaces are smooth, and crystallinity is good. SEM pictures were used to establish the average particle size and distribution at random[20]. Table 3 shows the mean particle sizes based on SEM images.

**Application of nanocomposite (corrosion protection):**

**Corrosion Test Cell**

Corrosion cell made of Pyrex with (1L) capacity Consists of two vessels, internal and external. The thermostat was used to make the temperature of seawater that flows through the outer vessel at (25, 35, 45 & 55) $^oC$. Three electrodes and a thermostat were replaced in the internal vessel. The three electrodes can be explained as the reference electrode, the Auxiliary, and the Working Electrode

Emulsion solution was prepared by adding 1% zinc oxide cobalt and oxide iron oxide nanocomposite powder to ethanol as solvent (adding 1.5 g nanocomposite to 150 ml ethanol). The emulsion solutions were applied to study the protection of C.S specimens by coating with nanocomposite by using EPD technique method

electrophoresis Deposition of $Co_3ZnFe_2O_8$ nanoparticles (Coating Samples) The date of corrosion parameters was inserted in table (4 )[21, 22]; this data shows the corrosion potential was shifted to more active potential when coated the surface of Carbon steel by $Co_3ZnFe_2O_8$ nanoparticles with water solvent[23]. It is clear from Figure (5) that $E_{corr}$ for the uncoated was shifted to a more active direction with increasing temperature from (293 to 313) K, while the corrosion of potential values was slightly affected by temperature when increased from 298 to 308 K for carbon steel coated by nanocomposite, therefore, return to (-718.2 µV) at 318K. Those indicate the mechanism of the C.S surface does not change by high temperature. The Protection Efficiency (%PE) can be calculated by using the equation (2) [23]:

$$\%PE = \frac{(i_{corr})\text{b} - (i_{corr})\text{p}}{(i_{corr})\text{b}} x\ 100 \ldots\ldots\ldots (2)$$

The $Co_3ZnFe_2O_8$ nanoparticles used as a coating for C.S reduce the corrosion from 168.71, 201.57, and 220.34 to 43.4, 48.3, and 61.5 µA.cm$^{-2}$ at 298, 308, and 318K, respectively. This reduces corrosion current due to getting protection efficiencies to reach 76.038% at 308K[24].

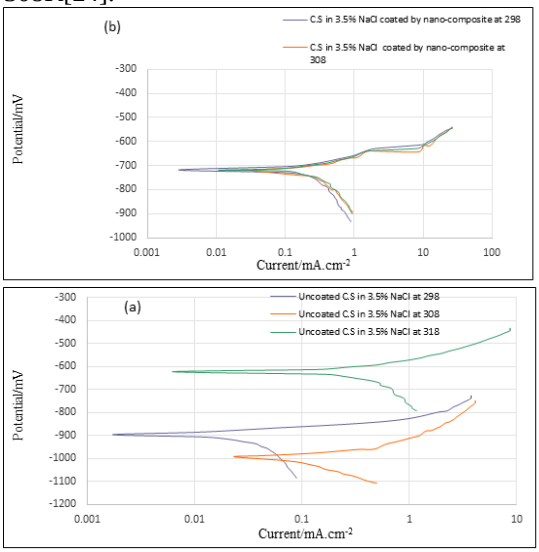


**Fig .5. Polarization curves for C.S a) Uncoated, b) Coated by nanoparticles**

**Table (4) corrosion parameters for C.S coated with $Co_3ZnFe_2O_8$ nanoparticles at different temperature**

| Carbon steel | T/K | -E corr /mV | $I_{corr}$/µA.cm$^{-2}$ | -bc/ V.dec$^{-1}$ | Ba /mV.dec$^{-1}$ | PE% | Θ |
|---|---|---|---|---|---|---|---|
| Un-coated | 298 | 469.0 | 168.72 | 243.9 | 107.2 | - | - |
| | 308 | 573.5 | 201.57 | 179.1 | 104.2 | - | - |
| | 318 | 622.0 | 220.34 | 140.3 | 82.2 | - | - |
| Coated | 298 | 718.6 | 43.4 | 104 | 13.9 | 74.2 | 0.742 |
| | 308 | 720.4 | 48.3 | 98.0 | 23.2 | 76.0 | 0.760 |
| | 318 | 718.8 | 61.5 | 82.7 | 26.3 | 72.0 | 0.720 |

## 5. Conclusion

In conclusion, novel $Co_3ZnFe_2O_8$ nanoparticles were successfully Synthesized by the photo Irradiation process and studied the optimum condition with different solvents; the smaller size and shape were with a solvent with water. To characterize synthesized Co3ZnFe2O8 nanoparticles, structural was studied by XRD and the crystalline size by Debye-Scherrer equation, scanning electron microscopy (SEM), and atomic force microscopy (AFM). These techniques prove that the nanocomposite size with water solvent was less than 70 nm, with chloroform solvent was103 nm, with methanol solvent was 96 nm, and with ethanol solvent was77 nm. The Protection Efficiency (%PE) can be calculated as 74% at 298.

## Acknowledgments

The authors would like to acknowledge Haider Abulkareem Al-Mashhdani and the University of Baghdad / College of Science / Department of Chemistry

## References

1. Abdulqawi, L.N.A. and S.A. Quadri, *Evaluation of Antibacterial and Antioxidant activities of Tribulus terrestris L. Fruits.* Research Journal of Pharmacy and Technology, 2021. **14**(1): p. 331-336.
2. Ismail, A.H., et al., *Synthesis, characterization, spectroscopic and biological studies of Zn (II), Mn (II) and Fe (II) theophylline complexes in nanoscale.* Nano Biomed. Eng, 2020. **12**(3): p. 253-61.
3. Aboud, N.A.-A., et al. *A comparative study of ZnO, CuO and a binary mixture of ZnO0. 5-CuO0. 5 with nano-dye on the efficiency of the dye-sensitized solar cell*. in *Journal of Physics: Conference Series*. 2020. IOP Publishing.
4. Kumar, S.S., et al., *Synthesis, characterization and optical properties of zinc oxide nanoparticles.* International Nano Letters, 2013. **3**(1): p. 1-6.
5. Nikam, A., B. Prasad, and A. Kulkarni, *Wet chemical synthesis of metal oxide nanoparticles:*

*A review.* CrystEngComm, 2018. **20**(35): p. 5091-5107.
6. Nikolova, M.P. and M.S. Chavali, *Metal oxide nanoparticles as biomedical materials.* Biomimetics, 2020. **5**(2): p. 27.
7. Siddiqi, K.S., A. ur Rahman, and A. Husen, *Properties of zinc oxide nanoparticles and their activity against microbes.* Nanoscale research letters, 2018. **13**(1): p. 1-13.
8. Abou El-Kheir, A. and L.K. El-Gabry, *Potential Applications of Nanotechnology In Functionalization of Synthetic Fibres (A Review).* Egyptian Journal of Chemistry, 2022. **65**(9): p. 5-6.
9. Sirelkhatim, A., et al., *Review on zinc oxide nanoparticles: antibacterial activity and toxicity mechanism.* Nano-micro letters, 2015. **7**(3): p. 219-242.
10. Abbas, H.A., K.A.S. Alsaade, and H.A.Y. AlMAshhdan. *Study the effect of cyperus rotundus extracted as mouthwash on the corrosion of dental amalgam*. in *IOP Conference Series: Materials Science and Engineering*. 2019. IOP Publishing.
11. Al-Jeilawi, U.H., S.M. Al-Majidi, and K.A. Al-Saadie, *Corrosion Inhibition Effects of Some New Synthesized N-Aroyl-N-Aryl thiourea Derivatives for Carbon Steel in Sulfuric Acid Media.* Al-Nahrain Journal of Science, 2013. **16**(4): p. 80-93.
12. AlMashhadani, H.A. *Corrosion Protection of Pure Titanium Implant by Electrochemical Deposition of Hydroxyapatite Post-Anodizing*. in *IOP Conference Series: Materials Science and Engineering*. 2019. IOP Publishing.
13. Al-Mashhadani, H.A., et al. *Anti-Corrosive Substance as Green Inhibitor for Carbon Steel in Saline and Acidic Media*. in *Journal of Physics: Conference Series*. 2021. IOP Publishing.
14. AlMashhadani, H.A. and K.A. Saleh, *Electro-polymerization of poly Eugenol on Ti and Ti alloy dental implant treatment by micro arc oxidation using as Anti-corrosion and Anti-microbial.* Res. J. Pharm. Technol, 2020. **13**(10): p. 4687.
15. Negash, Y., et al., *Antibacterial Activities of the CuO/ZnO Nanocomposite Grown on Silica Extracted from Bagasse Ash.* 2020.
16. Cui, H., et al., *The antibacterial activity of clove oil/chitosan nanoparticles embedded gelatin nanofibers against Escherichia coli O157: H7 biofilms on cucumber.* International journal of food microbiology, 2018. **266**: p. 69-78.
17. Gneedy, A.H., et al., *Application of marine algae separate and in combination with natural zeolite in dye adsorption from wastewater ; A review.* Egyptian Journal of Chemistry, 2022. **65**(9): p. 1-2.
18. Holzwarth, U. and N. Gibson, *The Scherrer equation versus the'Debye-Scherrer equation'.* Nature nanotechnology, 2011. **6**(9): p. 534-534.
19. Hammond, K., M.G. Ryadnov, and B.W. Hoogenboom, *Atomic force microscopy to elucidate how peptides disrupt membranes.* Biochimica et Biophysica Acta (BBA)-Biomembranes, 2021. **1863**(1): p. 183447.
20. Liang, J., et al., *Analytical Cryo-Scanning Electron Microscopy of Hydrated Polymers and Microgels.* Accounts of Chemical Research, 2021. **54**(10): p. 2386-2396.
21. El-Said Shehata, O., A.M. Abdel-karim, and A.H. Abdel Fatah, *New Trends in Anodizing and Electrolytic Coloring of Metals.* Egyptian Journal of Chemistry, 2022. **65**(9): p. 3-3.
22. AlMashhadani, H.A. and K.A. Saleh, *Electrochemical Deposition of Hydroxyapatite Co-Substituted By Sr/Mg Coating on Ti-6Al-4V ELI Dental Alloy Post-MAO as Anti-Corrosion.* Iraqi Journal of Science, 2020: p. 2751-2761.
23. Almashhdani, H. and K. Alsaadie, *Corrosion Protection of Carbon Steel in seawater by alumina nanoparticles with poly (acrylic acid) as charging agent.* Moroccan Journal of Chemistry, 2018. **6**(3): p. 6-3 (2018) 455-465.
24. Habib, S., R. Shakoor, and R. Kahraman, *A focused review on smart carriers tailored for corrosion protection: developments, applications, and challenges.* Progress in Organic Coatings, 2021. **154**: p. 106218.